There and back again – unraveling mechanisms of bacterial biogeography in the North Pacific Subtropical Gyre to and from station ALOHA

Markus V. Lindh[a†*]

[a]Daniel K. Inouye Center for Microbial Oceanography: Research and Education, University of Hawai'i at Mānoa, 1950 East West Road, Honolulu, Hawai'i, 96822, USA
[†]Present address: Department of Biology, Lund University, SE-22362, Sweden

*Corresponding author, *E-mail address*: markusvlindh@gmail.com

Keywords: Bacterial diversity, population dynamics, biogeography, metapopulation, colonization, extinction, core, satellite.

Running title: Bacterial metapopulation dynamics in the North Pacific Subtropical Gyre

Abstract

Bacterially-mediated fluxes of energy and matter are dynamic in time and space coupled with shifts in bacterial community structure. Yet, our understanding of mechanisms shaping bacterial biogeography remains limited. Near-surface seawater was collected during transits between Honolulu and Station ALOHA in the North Pacific Subtropical Gyre to examine the shape of occupancy-frequency distributions (the different number of populations occupying different number of sites) and determine bacterial metapopulation dynamics. Bacterial 16S rRNA gene amplicons were sequenced from whole seawater and filter-size fractionated plankton DNA samples while also separating the community into distinct taxonomic groups at phyla/class and analyzing these compartments separately. For the total seawater (i.e. the >0.2 µm size fraction) and picoplankton communities (i.e. the size fraction >0.2 µm and < 3.0 µm), but not the large size fraction community (i.e. the >3.0 µm size fraction), most individual operational taxonomic units (OTUs) occupied a single site and the number of OTUs occupying different number of sites followed a significant bimodal pattern with several core OTUs occupying all sites. Nevertheless, only Cyanobacteria (in particular *Prochlorococcus* sp.) and in a few instances also Alphaproteobacteria (in particular SAR11

clade and Aegan-169 marine group bacteria) exhibited bimodal occupancy-frequency patterns. As expected, *Prochlorococcus* sp. had an inversed bimodal occupancy-frequency distribution with most OTUs found at all sites. Yet, there were individual satellite OTUs affiliated with *Prochlorococcus* sp. that were phylogenetically distinct from the core OTUs and only found at a single site. Collectively, these findings indicate that different compartments (size fractions and taxa) have different metapopulation dynamics. Bimodal patterns among the low diversity total and picoplankton communities but not in the high diversity large size fraction suggest that positive feedbacks between local abundance and occupancy are important when environmental conditions are homogenous and diversity is low.

Introduction

Spatial and temporal variability in bacterial population dynamics influence nutrient cycling in aquatic systems (Crump et al., 2004; Kirchman et al., 2005; Fuhrman et al., 2006; Galand et al., 2010; Lindström et al., 2010; Östman et al., 2010; Alonso-Saez et al., 2015). Yet, despite observable biogeographical patterns among marine microbial assemblages (see e.g. Pommier et al., 2007; Ghiglione et al., 2012; Sunagawa et al., 2015; Salazar et al., 2016), the mechanisms shaping microbial biogeography remain largely unknown (Martiny et al., 2006; Hanson et al., 2012; Poisot et al., 2013).

With the introduction of high-throughput sequencing, and large sequence datasets enabled by these technologies, microbial ecologists are now able to test a wide variety of theoretical ecological models that are the foundation for mechanisms explaining macroecological patterns among larger taxa (Purdy et al., 2010; Poisot et al., 2013). Such theoretical models, including, but not limited to, metacommunity (Leibold et al., 2004) and metapopulation (McGeoch and Gaston, 2002) frameworks have provided mechanistic concepts in ecology among organisms ranging from birds to fish and insects to phytoplankton (Levin, 1974; Hanski, 1982; Gotelli, 1991; Tokeshi, 1992; Hanski and Gyllenberg, 1993; van Rensburg et al., 2000; Hubbell, 2001; Mehranvar and Jackson, 2001; Mouquet and Loreau M, 2002; Verberk et al., 2010; Unterseher et al., 2011; Wardle et al., 2011; Hercos et al., 2013).

Two models; Hanski's core and satellite hypothesis (CSH; (Hanski, 1982) and Levin's model (Levin, 1974), were recently empirically tested and used to explain distribution patterns among marine bacteria that are typically assumed not to be dispersal limited (Lindh et al., 2016). In the study bimodal occupancy-frequency patterns (i.e. the number of species occupying different number of sites) were found and the CSH model agreed well with observed data in the Baltic Sea and in global datasets, indicating its applicability also for marine microbes. The CSH model provides a mechanistic basis for the observation of

abundant (core) and rare (satellite) species in ecosystems. In brief, the CSH makes predictions of the shape of occupancy-frequency distributions from variation in colonization and extinction rates (i.e. populations successfully dispersed to previously unoccupied sites vs. populations disappearing from previously occupied sites). In the CSH the bimodal occupancy-frequency distributions are the result of stochastic variation in colonization and extinction rates (i.e. a quadratic relationship between colonization/extinction rates and occupancy) that either push populations to become rare or abundant. Nevertheless, empirical data from examining the applicability of metapopulation models to marine bacterial assemblages are limited.

In the present paper the prevalence of bimodal occupancy-frequency patterns were examined in the oligotrophic North Pacific Ocean and among different taxa and/or size fractions of a bacterial community. The main hypothesis was that in this relatively homogenous oligotrophic ocean environment bimodal patterns, reflecting a coherent oceanic region without dispersal limitation and environmental filtering, could be a common feature among marine bacteria. The second hypothesis was that taxa with different dispersal capability and filtered by various environmental conditions could display different metapopulation dynamics. The third hypothesis was that since *Prochlorococcus* sp. is the dominant bacteria found in this system (Schmidt et al., 1991; Campbell and Vaulot, 1993; Eiler et al., 2011) much of the observed metapopulation dynamics could be driven by this key organism but that there may be core- and satellite distribution patterns within the same genus. To test these hypotheses, bacterial 16S rRNA amplicons were sequenced from whole seawater and filter size fractionated community DNA, sampled from the near-surface ocean on a series of cruise transects between Honolulu and station ALOHA (22.75° N, 158° W) in the North Pacific Subtropical Gyre. The observed bacterial populations were subsequently fitted to different theoretical metapopulation models.

Material and Methods

Field sampling

Seawater samples for subsequent extraction of plankton DNA were collected during 4 research cruises (October 2015, HOT 277; November 2015, KM1519; December 2015, KM1521; and January 2016, HOT 280) offshore of the Hawaiian island of Oahu aboard the R/V Ka'imikai-O-kanaloa and R/V *Kilo Moana*. Seawater was collected from the research vessels' flow-through seawater intake systems into acid-washed, Milli-Q rinsed polycarbonate bottles. The flow-through seawater system was instrumented to include a thermosalinometer (SeaBird 911), fluorometer (Seapoint Chlorophyll Fluorometer; Seapoint Sensors, Inc.) and dissolved oxygen (O_2) sensor (SBE 43; Sea-Bird Electronics). On all cruises, plankton biomass for subsequent DNA extraction was harvested by filtering 2 L of seawater on to 25 mm diameter, 0.2 µm pore size polyethersulfone filters (Supor membrane, Pall). In addition, on two of the cruises (December 2015 and January 2016) plankton biomass were also sequentially filter size-fractionated samples for subsequent extraction of DNA for information on bacterial community structure among different plankton size classes. During these cruises, seawater was filtered onto 25 mm diameter, 3.0 µm pore size polycarbonate membranes (Millipore), followed by filtration onto 25 mm diameter, 0.2 µm pore size Supor filters. The various filter size-fractionated bacterial communities were defined as: total (>0.2 µm), picoplankton (>0.2 and <3 µm) and large (>3 µm), respectively. Filters were stored at -80°C until extraction.

Coincident samples for measurement of bacterial abundance and production were collected from the vessels' flow-through seawater system. Seawater for determination of bacterial abundance was subsampled into 2 ml cryotubes (BD Falcon) preserved with 20 µL paraformaldehyde (Final concentration 0.2%; Sigma-Aldrich). Triplicate 1.5 ml samples for subsequent measurements of ^{3}H-leucine incorporation rates were aliquoted into 2.0 ml

119 microcentrifuge tubes (Axygen; (Pace et al., 2004)) and amended with 20 nM (final
120 concentration) of ^{3}H-leucine stock (3, 4, 5 -^{3}H-leucine, 109 Ci/mmol; Perkin-Elmer). One
121 killed control was included from each station sampled (5% final concentration of
122 trichloroacetic acid; Sigma-Aldrich). Samples for ^{3}H-leucine incorporation rates were
123 incubated shipboard at *in situ* temperatures following the ^{3}H-leucine incorporation protocol
124 described in (Kirchman et al., 1985) and (Smith and Azam, 1992). Preserved bacterial
125 abundance and killed ^{3}H-leucine incorporation rate samples were flash frozen in liquid
126 nitrogen and stored at -80° C until processing in the laboratory. Preserved bacterial abundance
127 samples were thawed, and aliquoted into 250 µl wells and stained with 2.5µl µl of 100X
128 SybrGreen (Thermo Fisher) and enumerated using an Attune™ acoustic focusing flow
129 cytometer (Applied Biosystems). ^{3}H-leucine incorporation rates samples were processed
130 following a modified method of the microcentrifuge method as described in (Smith and
131 Azam, 1992). A detailed description of the ^{3}H-leucine incorporation protocol can be found in
132 (Viviani and Church, 2017).
133
134 *DNA extraction, PCR, sequence processing and analysis.*
135 DNA was extracted from the filters using the DNeasy Plant MiniKit (Qiagen) following slight
136 modifications of the manufacturer's suggestions. Modifications included the addition of
137 Proteinase K to the lysis buffer followed by bead-beating with 0.1 mm and 0.5 mm glass beads
138 (Biospec products) for additional cell disruption prior to the extraction. DNA concentrations were
139 determined using the Qubit 2.0 Fluorometer and Qubit dsDNA High Sensitivity Assay kit
140 (Molecular Probes), with DNA quality checked using 1.5% agarose gel electrophoresis. Extracted
141 DNA was stored at -80°C.
142 Amplicon processing for all samples was performed as described in (Lindh et al., 2015).
143 Bacterial 16S rRNA was amplified using primers 341F and 805R (Herlemann et al., 2011)

144 following the PCR protocol of (Hugerth et al., 2014). Amplicons were purified by spin-column
145 centrifugation using E.Z.N.A.® Cycle Pure kit (Omega Biotek). The resulting purified amplicons
146 were pooled in equimolar concentration and sequenced on an Illumina Miseq (Illumina, USA)
147 platform at the Hawai'i Institute for Marine Biology (HIMB), Hawaii, USA using the 300 bp
148 paired-end setting. Raw sequence data generated from Illumina Miseq were processed using the
149 UPARSE pipeline (Edgar, 2013). Taxonomy was determined against the SINA/SILVA database
150 (SILVA123; (Quast et al., 2013)). After quality filtering and discarding plastid and archaeal
151 sequences a total of 1.25 million bacterial sequences were utilized for subsequent analyses. Thus,
152 the final OTU table consisted of 96 samples with 27340 OTUs delineated at 99% 16S rRNA gene
153 identity with an average of 13093±5644 sequences per sample. For all alpha diversity measures
154 the OTU table were subsampled to 10,000 sequences per sample. DNA sequences have been
155 deposited in the National Center for Biotechnology Information (NCBI) Sequence Read Archive
156 under accession number SRP091841.
157
158 *Statistical tests*
159 Occupancy-frequency distributions (the number of OTUs occupying different
160 number of sites) were analyzed as described in (Lindh et al., 2016). In brief, an equivalent to
161 Tokeshi's test of bimodality was performed using Mitchell-Olds' and Shaw's test (Mitchell-
162 Olds and Shaw, 1987) for the location of quadratic extremes. Colonization and extinction
163 rates of OTUs were determined by calculating the change in fraction of sites occupied
164 between two cruises where the same stations were sampled with <1 month interval. Non-
165 linear least squares analysis of observed colonization and extinction rates was performed
166 using the equations of Levin's model, the CSH hypothesis and Gotelli's propagule rain model
167 (Levin, 1974; Hanski, 1982; Gotelli, 1991).
168 All statistical tests were performed in R 3.3.3 (Team, 2014) using the package "Vegan"

(Jari Oksanen et al., 2010). Graphical outputs were made in R 3.3.3 using the package "ggplot2" (Wickham, 2009).

Results

In the present study bacterial population dynamics and biogeography were examined during 4 research cruises in the North Pacific Subtropical Gyre (Fig. 1). For all four transects (total 96 samples) 27,340 operational taxonomic units (OTUs) were detected. A more exhaustive sampling was performed in the October 2015 cruise with measurements of a larger set of biotic and abiotic measurements and is thus the focus in the present paper. An additional cruise with a different transect (November 2015) to the Southwest of Oahu were performed to compare patterns observed in the October 2015 cruise. Finally, on two cruises (December 2015 and January 2016), samples were filter size-fractionated for information on bacterial diversity associated with differing size classes of plankton (>3 µm, >0.2 and <3.0 µm, and >0.2 µm, large, picoplankton and total, respectively).

Physicochemical conditions, community abundance, production and biodiversity

Across the 200 km transect to Station ALOHA (October 2015) concentrations of Chl *a* and sea surface temperatures were relatively stable in space, averaging 0.6 µg L^{-1} and 26°C, respectively (Fig. 2). Bacterial abundance varied ~2-fold (ranging 5.73 x10^5 cells ml^{-1} to 9.13 x10^5 cells ml^{-1}; Fig. 2). ^{3}H-leucine incorporation rates ranged between 13 and 37 pmol Leu L^{-1} h^{-1} (Fig. 2). Variation in bacterial abundance and production was overall small (SD = 0.7 x10^5 cells ml^{-1} and SD = 6 pmol Leu L^{-1} h^{-1}; Fig. 2).

The number of OTUs varied between 371 and 1037 but appeared relatively stable in space and time (SD = 145.34). Estimation of alpha diversity followed a similar trend where Shannon diversity index and Chao 1 richness varied between 3.99 and 5.06and 903.45

194 to 2256.88, respectively. Alpha diversity for the total community was also stable within all
195 other cruises around the same range as observed during October 2015 (Fig. S1A). During the
196 December 2015 and January 2016 transect, size fractionation of plankton DNA samples
197 revealed higher alpha diversity in the larger size fraction (3.0 µm filter fraction) compared to
198 the total (>0.2 µm) and picoplankton fraction (0.2 and 3.0 µm; Fig. S1A).
199
200 *Bacterial community composition*
201 In all cruises the total and picoplankton communities were dominated by Cyanobacteria
202 (averaging ~50% of total sequences), with bacteria that were affiliated with several other
203 phyla or classes not included in the taxonomic analysis or unclassified OTUs comprising
204 nearly 25% of the total sequences (Fig. 3). Actinobacteria and Alphaproteobacteria each
205 typically contributed to ~5% of total sequences in these communities. In the December 2015
206 and January 2016 cruises the large size class bacterial assemblages were more diverse than
207 other size classes of bacteria, with notable increases in relative abundances of
208 Alphaproteobacteria, Planctomycetes, Chloroflexi and Bacteroidetes (Fig. 3B). However,
209 Cyanobacteria were also dominating the large size class communities. Cluster analysis of
210 Bray-Curtis distances obtained from samples in the October 2015 cruise showed a largely
211 similar community structure (~15% dissimilarity), resulting in samples from near-shore
212 coastal sites clustering with samples from the open ocean sites (Fig. 3).
213 Among the top ten most abundant OTUs all were affiliated with
214 *Prochlorococcus* sp., demonstrating homogenous relative abundances along the transect (Fig
215 S2). Other less abundant OTUs that exhibited variance in relative abundance along the
216 transect, included the OM-1 clade bacteria (*Candidatus* Actinomarina) and OTUs within the
217 family *Rhodospirillaceae* affiliated with AEGEAN-169 marine group. Notably, the OM-1
218 clade bacteria appeared relatively enriched in a localized region north of Oahu (22° N, see

arrows Fig. S3). Nevertheless, the variation in relative abundance among these OTUs was low.

Occupancy-frequency distributions

The number of different species occupying different number of sites sampled during the transects were also examined to evaluate the shape of occupancy-frequency distributions. Bacterial communities sampled during the October 2015 cruise displayed a significant bimodal occupancy-frequency pattern. Most OTUs were found at a single site followed by a monotonical decrease in the number of OTUs occupying increasing number of sites but with a peak in the number of OTUs occupying all sites (Fig. 4A; Table S1). As this transect contained several samples obtained from around Station ALOHA this dataset were subsampled to only show stations 3, 6, 9, 13, 33 and 47 to keep a clear transect trajectory profile with distinct sites (see insert Fig. 4A). This subsampling exercise confirmed the significant bimodal pattern. In addition, samples from completely different stations in a trajectory 30 km Southeast of Honolulu were collected to validate the shape of occupancy-frequency distribution found in the Honolulu-Station ALOHA transect. Also for this transect a significant bimodal pattern were found (see insert Fig. 4A).

The main hypotheses were that different parts of a bacterial community may exhibit different metapopulation dynamics; for example, taxa distributed among the picoplankton and larger bacterial assemblages might have different dispersal capabilities and be subjected to different environmental filters. To elucidate differences between such compartments the total community from the October 2015 cruise and size-fractionated communities from the December 2015 and January 2016 cruises were examined and taxa were analyzed at different taxonomic levels. Similar to the "total" community, the picoplankton assemblage demonstrated significant bimodal patterns (Fig. 4B; Table S1); in

contrast, for the "large" bacterial size classes most OTUs were found at a single site followed by a monotonical decrease in the number of OTUs occupying increasing number of sites. Thus, in contrast to the picoplankton and total communities, the large size fractions exhibited unimodal occupancy-frequency patterns (Fig. 4B; Table S1). In addition, for particular OTUs binned at the phyla/class level detected in the October 2015 cruise varying occupancy-frequency distributions were observed. In fact, only Planctomycetes, Alphaproteobacteria, and Cyanobacteria contained OTUs that were found at all sites and only the latter two displayed bimodal patterns (Fig. S4; Table S1). Cyanobacteria had the most substantial bimodal pattern with a strong peak in number of OTUs occupying all sites. Moreover, most OTUs binned at the phyla/class level exhibited unimodal patterns for picoplankton and large size class communities (Fig. S5; Table S1).

More than 50% (64 out of 108) of the core OTUs detected from the October 2015 cruise was affiliated with *Prochlorococcus* sp. (Fig. 3; S6A). When analyzed separately, *Prochlorococcus* sp. OTUs exhibited a strong right-skewed occupancy-frequency distribution in the total and picoplankton size classes, with most OTUs occupying all sites. There were satellite phylotypes among the *Prochlorococcus* sp. affiliated OTUs detected at only a single site (Fig. S6). Notably, for the *Prochlorococcus* sp. OTUs in the large size class communities, neither unimodal nor bimodal occupancy-frequency patterns were detected (Fig. S6B). By analyzing phylogenetically distinct *Prochlorococcus* sp. OTUs and comparing those OTUs detected at all sites (core) vs. the OTUs only found in a single site (satellite) phylogenetic differences in core/satellite characteristics among closely related populations were examined. This analysis revealed that the most abundant core *Prochlorococcus* sp. OTUs were phylogenetically distinct from the most frequently observed satellite OTUs within the same genus (Fig. S7).

Colonization and extinction rates

In the CSH (Hanski, 1982) predicted bimodal occupancy-frequency distributions of species based on stochastic variation in colonization and extinction rates following a quadratic relationship between these rates and occupancy. By calculating the number of OTUs successfully dispersed to new sites compared to the number of OTUs that disappeared from occupied sites colonization and extinction rates was estimated (Fig. 5). These calculations were performed using the December 2015 and January 2016 cruises where the same stations were sampled allowing for the observation of temporal changes in the number of occupied sites (d*P*/dt).

The total bacterial community was characterized by a quadratic curve for both colonization and extinction rates. Notably, extinction rates were higher than colonization rates with a more distinct quadratic curve (Fig. 5A). Both colonization and extinction rates fitted well with the quadratic relationship described by the CSH (Hanski, 1982). For the picoplankton and large size class communities, the relationship between colonization rates and occupancy were more difficult to determine and none of the models tested resulted in robust fits to the observations (Fig. 5A). However, for the large plankton size class, extinction rates aligned well with the expectation of a linear relationship between extinction rates and occupancy as described in Levin's model (Levin, 1974).

At the Phyla/Class level rates of colonization and extinction were plotted against occupancy for major bacterial lineages (Fig. 5B). Both Alphaproteobacteria and Cyanobacteria demonstrated quadratic relationships between extinction rates and occupancy in the total community. However, as above, colonization rates were more difficult to characterize. It was noteworthy that the extinction rates were both higher and more pronounced compared to colonization rates. Planctomycetes, Bacteroidetes and Gammaproteobacteria demonstrated curves that initially appeared to follow a quadratic

294 relationship between extinction rates and occupancy, but either decreased followed by an
295 increase in extinction rates with occupancy (Planctomycetes and Gammaproteobacteria)
296 and/or did not decrease rapidly at maximum occupancy (Bacteroidetes). Unlike the patterns
297 for all of the OTUs in the overall community analysis, resulting patterns among the
298 picoplankton and large size class bacterial communities at phyla/class level were more
299 difficult to validate using the different metapopulation models. Nevertheless, extinction rates
300 among OTUs binned at phyla/class for the larger size class communities displayed a tendency
301 toward a linear relationship between extinction rates and occupancy thus following Levin's
302 model (Levin, 1974) (Fig. 5B).
303
304 **Discussion**
305 In the present paper metapopulation models were applied to describe bacterial
306 community dynamics observed in the North Pacific Subtropical Gyre to elucidate
307 mechanisms shaping biogeography. The results highlight that bimodal occupancy-frequency
308 patterns are prominent in the North Pacific Subtropical Gyre but only among specific size
309 classes and taxa of the bacterial communities. Total (≥0.2 µm size fraction) and
310 picoplanktonic (≥0.2 µm ≤3.0 µm size fraction) communities typically displayed bimodal
311 patterns, whereas the larger size class (≥3.0 µm filter fraction) community exhibited unimodal
312 patterns. In instances where bimodal patterns were found quadratic relationships between
313 rates of colonization/extinction and occupancy were observed. These findings indicate a
314 strong positive feedback mechanism between local abundance and occupancy and the
315 observed patterns generally fit Hanski's metapopulation model, the CSH (Hanski, 1982). In
316 agreement, significant bimodal occupancy-frequency distributions linked with quadratic
317 colonization and extinction rates have been found among bacterial assemblages in the Baltic
318 Sea Proper (Lindh et al., 2016).

Environmental conditions and diversity regulate metapopulation dynamics

Concomitant measurements of environmental variables, bacterial abundance and ^{3}H-leucine incorporation rates in the present paper allowed for linking mechanisms shaping biogeography with the prevailing environmental conditions and community functioning. Overall, the environment and community dynamics was highly stable throughout each of the transects performed coupled with core and satellite metapopulation dynamics. Bimodal patterns were typically coupled with lower community diversity and quadratic relationships between colonization/extinction rates and occupancy of OTUs in the total and picoplankton communities. In contrast, the large size fraction communities exhibited unimodal patterns linked with higher diversity and linear colonization and extinction rates of OTUs. These data suggest that positive feedbacks between local abundance and occupancy are important in structuring picoplankton bacterial communities when environmental conditions are homogenous and diversity is low. Still, it is noteworthy that the metadata in this study was derived from whole seawater and total community and the environmental conditions characterizing the size fractionated "large" communities are unknown. Further more focused studies coupling size fractionated community composition and functioning would be very rewarding for our understanding of metapopulation dynamics and ultimately provide a deeper mechanistic understanding of biogeography of both picoplankton and large size fraction communities.

Metapopulation dynamics of Prochlorococcus sp.

OTUs affiliated with *Prochlorococcus* sp. contributed up to 50 % of total sequences for the total and picoplankton communities. A majority of the detected core populations were in fact affiliated with *Prochlorococcus* sp., thus driving much of the

344 observed metapopulation dynamics. In agreement with these findings, *Prochlorococcus* sp. is
345 the dominant bacteria found in this system (Schmidt et al., 1991; Campbell and Vaulot, 1993;
346 Eiler et al., 2011) and are ubiquitous in the oligotrophic ocean (Flombaum et al., 2013).
347 However, this is the first study to examine metapopulation models for *Prochlorococcus* sp.
348 and finding core- and satellite dynamics for this key organism. Although many of the
349 *Prochlorococcus* sp. OTUs found in this study were distributed over all stations, OTUs within
350 the same taxa had more restricted ranges geographically. Such OTUs with restricted
351 distributions also added to the dominance of the left-skewed majority of rare satellite
352 populations indicating dispersal and environmental filtering of particular *Prochlorococcus*
353 ecotypes. Although this bacterium is ubiquitously distributed in the oligotrophic surface
354 ocean, ecotypes within the same species have been suggested from variations in genome
355 content and functional potential (Rocap et al., 2003). In fact, ecotypes of *Prochlorococcus* sp.
356 have been observed in the Atlantic Ocean along environmental gradients with varying
357 conditions implicating niche partitioning of closely related 16S rRNA sequences derived from
358 the same species (Johnson et al., 2006). Single-cell genomic approaches have further
359 emphasized that subpopulations of the same *Prochlorococcus* sp. are likely adapted to
360 different environmental conditions (Kashtan et al., 2014). Taken together, *Prochlorococcus*
361 sp. metapopulations exhibited core and satellite dynamics indicative of positive feedback
362 mechanisms between local abundance and occupancy suggesting a rescue effect of core
363 populations (Hanski, 1982; Hanski and Gyllenberg, 1993).
364
365 *Disentangling community compartments*
366 Individual taxonomic groups and particular OTUs displayed different metapopulation
367 dynamics suggesting that taxa likely have different dispersal capability and are subjected to
368 environmental filtering. Further studies at deeper taxonomic levels are however warranted to

examine dynamics of "large" communities at different spatial scales to determine the mechanisms that regulate their biogeographical distribution. From observing variation in the shape of occupancy-frequency distributions among complex assemblages studied in macroecology (Mehranvar and Jackson, 2001) and colleagues have suggested that pooling all taxa into the same metapopulation model obscured taxonomic differences. Such taxonomic differences in compartments of communities may ultimately be linked with different dispersal capabilities and assembly of distinct species (Lindström and Langenheder, 2012). Conclusions made on community structure from high-throughput sequencing of microbial assemblages coupled with community functioning should thus be done with care and relative to individual compartments.

Acknowledgements

I acknowledge Matthew Church for valuable support and for providing comments on the paper, the HOT program science team for their assistance at sea, in the lab and for providing contextual data used in this study. In addition, I thank the captain, officers, and crew of the R/V *Ka'imikai-O-Kanaloa* and *Kilo Moana* for their assistance on the cruises. I am also grateful to Lance Fujieki for his assistance with CTD data processing. Funding for this research derived from the Simons Collaboration on Ocean Processes and Ecology (SCOPE) to Matthew Church.

References

Alonso-Saez, L., Diaz-Perez, L., and Moran, X.A. (2015) The hidden seasonality of the rare biosphere in coastal marine bacterioplankton. *Environ Microbiol* **17**: 3766-3780.

Brown, J.H. (1984) On the relationship between abundance and distribution of species *American Naturalist* **124**: 255-279.

394 Campbell, L., and Vaulot, D. (1993) Photosynthetic picoplankton community structure in the
395 subtropical North Pacific Ocean near Hawaii (station ALOHA). *Deep Sea Res*
396 *Pt I* **40**: 2043-2060.
397 Crump, B.C., Hopkinson, C.S., Sogin, M.L., and Hobbie, J.E. (2004) Microbial Biogeography
398 along an Estuarine Salinity Gradient: Combined Influences of Bacterial Growth
399 and Residence Time. *Appl Environ Microbiol* **70**: 1494-1505.
400 Edgar, R.C. (2013) UPARSE: highly accurate OTU sequences from microbial amplicon
401 reads. *Nat Methods* **10**: 996-998.
402 Eiler, A., Hayakawa, D., and Rappé, M. (2011) Non-Random Assembly of Bacterioplankton
403 Communities in the Subtropical North Pacific Ocean. *Front Microbiol* **2**.
404 Felsenstein, J. (1985) Confidence Limits on Phylogenies: An Approach Using the Bootstrap.
405 *Evolution* **39**: 783-791.
406 Flombaum, P., Gallegos, J.L., Gordillo, R.A., Rincón, J., Zabala, L.L., Jiao, N. et al. (2013)
407 Present and future global distributions of the marine Cyanobacteria
408 Prochlorococcus and Synechococcus. *Proc Natl Acad Sci USA* **110**: 9824-9829.
409 Fuhrman, J.A., Hewson, I., Schwalbach, M.S., Steele, J.A., Brown, M.V., and Naeem, S.
410 (2006) Annually reoccurring bacterial communities are predictable from ocean
411 conditions. *Proc Natl Acad Sci USA* **103**: 13104-13109.
412 Galand, P.E., Potvin, M., Casamayor, E.O., and Lovejoy, C. (2010) Hydrography shapes
413 bacterial biogeography of the deep Arctic Ocean. *ISME J* **4**: 564-576.
414 Ghiglione, J.F., Galand, P.E., Pommier, T., Pedros-Alio, C., Maas, E.W., Bakker, K. et al.
415 (2012) Pole-to-pole biogeography of surface and deep marine bacterial
416 communities. *Proc Natl Acad Sci USA* **109**: 17633-17638.
417 Gotelli, N.J. (1991) Metapopulation models: the rescue effect, the propagule rain, and the
418 core-satellite hypothesis. *Am Nat* **X**: 768-776.

419 Hanski, I. (1982) Dynamics of regional distribution - the core and satellite species hypothesis.
420 *Oikos* **38**: 210-221.
421 Hanski, I., and Gyllenberg, M. (1993) Two General Metapopulation Models and the Core-
422 Satellite Species Hypothesis. *Am Nat* **142**: 17-41.
423 Hanson, C.A., Fuhrman, J.A., Horner-Devine, M.C., and Martiny, J.B. (2012) Beyond
424 biogeographic patterns: processes shaping the microbial landscape. *Nat Rev*
425 *Microbiol* **10**: 497-506.
426 Hercos, A.P., Sobansky, M., Queiroz, H.L., and Magurran, A.E. (2013) Local and regional
427 rarity in a diverse tropical fish assemblage. *Paper* **Vol**: Page.
428 Herlemann, D.P., Labrenz, M., Jurgens, K., Bertilsson, S., Waniek, J.J., and Andersson, A.F.
429 (2011) Transitions in bacterial communities along the 2000 km salinity gradient
430 of the Baltic Sea. *ISME J* **Vol**: Page.
431 Hubbell, S.P. (2001) The unified neutral theory of biodiversity and biogeography (MPB-32):
432 Princeton University Press.
433 Hugerth, L.W., Wefer, H.A., Lundin, S., Jakobsson, H.E., Lindberg, M., Rodin, S. et al.
434 (2014) DegePrime, a program for degenerate primer design for broad-
435 taxonomic-range PCR in microbial ecology studies. *Appl Environ Microbiol* **80**:
436 5116-5123.
437 Johnson, Z.I., Zinser, E.R., Coe, A., McNulty, N.P., Woodward, E.M.S., and Chisholm, S.W.
438 (2006) Niche Partitioning Among Prochlorococcus Ecotypes Along Ocean-
439 Scale Environmental Gradients. *Science* **311**: 1737-1740.
440 Kashtan, N., Roggensack, S.E., Rodrigue, S., Thompson, J.W., Biller, S.J., Coe, A. et al.
441 (2014) Single-Cell Genomics Reveals Hundreds of Coexisting Subpopulations
442 in Wild Prochlorococcus. *Science* **344**: 416-420.
443 Kirchman, D., K'Ness, E., and Hodson, R. (1985) Leucine incorporation and its potential as a

444 measure of protein synthesis by bacteria in natural aquatic systems. *Appl*
445 *Environ Microbiol* **49**: 599-607.
446 Kirchman, D.L., Dittel, A.I., Malmstrom, R.R., and Cottrell, M.T. (2005) Biogeography of
447 major bacterial groups in the Delaware Estuary. Limn Oceanogr **50**: 1697-1706.
448 Kumar, S., Stecher, G., and Tamura, K. (2016) MEGA7: Molecular Evolutionary Genetics
449 Analysis version 7.0 for bigger datasets. *Molecular Biology and Evolution*.
450 Leibold, M.A., Holyoak, M., Mouquet, N., Amarasekare, P., Chase, J.M., Hoopes, M.F. et al.
451 (2004) The metacommunity concept: a framework for multi-scale community
452 ecology. *Ecol Lett* **7**: 601-613.
453 Levin, S.A. (1974) Dispersion and population interactions *Am Nat* 108: 207-228.
454 Lindh, M.V., Figueroa, D., Sjöstedt, J., Baltar, F., Lundin, D., Andersson, A. et al. (2015)
455 Transplant experiments uncover Baltic Sea basin-specific responses in
456 bacterioplankton community composition and metabolic activities. *Front*
457 *Microbiol* **6**: Page.
458 Lindh, M.V., Sjöstedt, J., Ekstam, B., Casini, M., Lundin, D., Hugerth, L.W. et al. (2016)
459 Metapopulation theory identifies biogeographical patterns among core and
460 satellite marine bacteria scaling from tens to thousands of kilometers. *Environ*
461 *Microbiol* Vol: Page..
462 Lindström, E.S., and Langenheder, S. (2012) Local and regional factors influencing bacterial
463 community assembly. *Environ Microbiol Rep* **4**: 1-9.
464 Lindström, E.S., Feng, X.M., Graneli, W., and Kritzberg, E.S. (2010) The interplay between
465 bacterial community composition and the environment determining function of
466 inland water bacteria. *Limnol Oceanogr* **55**: 2052-2060.
467 Martiny, J.B.H., Bohannan, B.J.M., Brown, J.H., Colwell, R.K., Fuhrman, J.A., Green, J.L. et
468 al. (2006) Microbial biogeography: putting microorganisms on the map. *Nat Rev*

Microbiol **4**: 102-112.

McGeoch, M.A., and Gaston, K.J. (2002) Occupancy frequency distributions: patterns, artefacts and mechanisms. *Biol Rev* **77**: 311-331.

Mehranvar, L., and Jackson, D.A. (2001) History and taxonomy: their roles in the core-satellite hypothesis. *Oecologia* **127**: 131-142.

Mitchell-Olds, T., and Shaw, R.G. (1987) Regression Analysis of Natural Selection: Statistical Inference and Biological Interpretation. *Evolution* **41**: 1149-1161.

Mouquet, N., and Loreau M (2002) Coexistence in Metacommunities: The Regional Similarity Hypothesis. *Am Nat* **159**: 420-426.

Oksanen, J., Guillaume Blanchet, F., Kindt, R., Legendre, Pierre., O'Hara, R. B., Simpson G. L., et al. (2010) vegan: Community Ecology Package. R package version 1.17-5. https://cran.r-project.org/web/packages/vegan/index.html.

Pace, M.L., del Giorgio, P., Fischer, D., Condon, R., and Malcom, H. (2004) Estimates of bacterial production using the leucine incorporation method are influenced by differences in protein retention of microcentrifuge tubes. *Limnol Oceanogr Meth* **2**: 55-61.

Poisot, T., Pequin, B., and Gravel, D. (2013) High-throughput sequencing: a roadmap toward community ecology. *Ecol Evol* **3**: 1125-1139.

Pommier, T., Canback, B., Riemann, L., Bostrom, K.H., Simu, K., Lundberg, P. et al. (2007) Global patterns of diversity and community structure in marine bacterioplankton. *Mol Ecol* **16**: 867-880.

Purdy, K.J., Hurd, P.J., Moya-Larano, J., Trimmer, M., Oakley, B.B., Woodward, G., and Guy, W. (2010) Systems biology for ecology: from molecules to ecosystems. *Adv Ecol Res* **43**: 87-149.

Quast, C., Pruesse, E., Yilmaz, P., Gerken, J., Schweer, T., Yarza, P. et al. (2013) The SILVA

494 ribosomal RNA gene database project: improved data processing and web-based
495 tools. *Nucl Acids Res* **41**: D590-596.
496 R Core Team. (2014) R: A Language and Environment for Statistical Computing.
497 https://cran.r-project.org/
498 Rocap, G., Larimer, F.W., Lamerdin, J., Malfatti, S., Chain, P., Ahlgren, N.A. et al. (2003)
499 Genome divergence in two Prochlorococcus ecotypes reflects oceanic niche
500 differentiation. *Nature* **424**: 1042-1047.
501 Salazar, G., Cornejo-Castillo, F.M., Benitez-Barrios, V., Fraile-Nuez, E., Alvarez-Salgado,
502 X.A., Duarte, C.M. et al. (2016) Global diversity and biogeography of deep-sea
503 pelagic prokaryotes. *ISME J* **10**: 596-608.
504 Schmidt, T.M., DeLong, E.F., and Pace, N.R. (1991) Analysis of a marine picoplankton
505 community by 16S rRNA gene cloning and sequencing. *J Bacteriol* **173**: 4371-
506 4378.
507 Smith, D.C., and Azam, F. (1992) A simple, economical method for measuring bacterial
508 protein synthesis rates in seawater using 3H-leucine. *Marine Microb Food Webs*
509 **6**: 107-114.
510 Sunagawa, S., Coelho, L.P., Chaffron, S., Kultima, J.R., Labadie, K., Salazar, G. et al. (2015)
511 Structure and function of the global ocean microbiome. *Science* **348**: Page**.**
512 Tamura, K., and Nei, M. (1993) Estimation of the number of nucleotide substitutions in the
513 control region of mitochondrial DNA in humans and chimpanzees. *Mol Biol*
514 *Evol* **10**: 512-526.
515 Tokeshi, M. (1992) Dynamics of distribution in animal communities - theory and analysis.
516 *Res Pop Ecol* **34**: 249-273.
517 Unterseher, M., Jumpponen, A.R.I., ÖPik, M., Tedersoo, L., Moora, M., Dormann, C.F., and
518 Schnittler, M. (2011) Species abundance distributions and richness estimations

519 in fungal metagenomics – lessons learned from community ecology. *Mol Ecol*
520 **20**: 275-285.
521 van Rensburg, B.J., McGeoch, M.A., Matthews, W., Chown, S.L., and van Jaarsveld, A.S.
522 (2000) Testing generalities in the shape of patch occupancy frequency
523 distributions *Ecology* **81**: 3163-3177.
524 Verberk, W.C.E.P., Van Der Velde, G., and Esselink, H. (2010) Explaining abundance–
525 occupancy relationships in specialists and generalists: a case study on aquatic
526 macroinvertebrates in standing waters. *JAnim Ecol* **79**: 589-601.
527 Viviani, D.A., and Church, M.J. (2017) Decoupling between bacterial production and primary
528 production over multiple time scales in the North Pacific Subtropical Gyre.
529 *Deep Sea Res Pt I* **121**: 132-142.
530 Wardle, D.A., Bardgett, R.D., Callaway, R.M., and Van der Putten, W.H. (2011) Terrestrial
531 Ecosystem Responses to Species Gains and Losses. *Science* **332**: 1273-1277.
532 Wickham, H. (2009) ggplot2: elegant graphics for data analysis. New York: Springer.
533 Östman, O., Drakare, S., Kritzberg, E.S., Langenheder, S., Logue, J.B., and Lindström, E.S.
534 (2010) Regional invariance among microbial communities. *Ecol Lett* **13**: 118-
535 127.
536

537 **Figures and Tables**

538 **Figure 1.** Map illustrating the four transects performed with the locations of Station ALOHA
539 and Station Kahe marked. Asterisks denote the same station sample repeatedly.
540

541 **Figure 2.** Variation bacterial community abundance, production and alpha diversity during
542 the October 2015 cruise, including variation in Chl *a* (green open circles) and average sea
543 surface temperature (blue dotted line).

Figure 3. Variation in community composition during the October 2015 cruise (A), and November 2015, December 2015 and January 2016 cruises (B). Barcharts denote relative abundance (% of total sequences) among major bacterial groups at phyla/class. Dendrogram in (A) denote cluster analysis of variation in beta diversity estimated from Bray-Curtis distances. For the cruises in December 2015 and January 2016 in (B) total, picoplankton and "large" denote size-fractionated community DNA from >0.2 µm, >0.2 and <3.0 µm and 3.0 µm filters, respectively.

Figure 4. Core and satellite populations detected among occupancy-frequency distributions during the October 2015 cruise (A), and December 2015 and January 2016 cruises (B). Insert in (A) shows occupancy-frequency distributions of populations in a subset of the October 2015 cruise with the same stations sampled in the December 2015 and January 2016 cruises and the additional cruise in November 2015. Total, picoplankton and "large" denote size-fractionated community DNA from >0.2 µm, >0.2 and <3.0 µm and 3.0 µm filters, respectively. The y-axis is scaled at maximum 500 OTUs. Bimodality tests was performed using Mitchell-Olds and Shaw's test for quadratic extremes (Mitchell-Olds and Shaw, 1987), a proxy for Tokeshi's test (Tokeshi, 1992). ND=Not Determined. Significance level is indicated with "***", "**" and"*" for p-values <0.001, <0.01 and <0.05, respectively.

Figure 5. Measured colonization and extinction rates for all OTUs collectively (A), and for all OTUs within major bacterial groups and particular OTUs within the same genus (B). Observed rates in (A) were fitted with theoretical predictions from different metapopulation models.

Supporting information

Supplementary Figures and Tables

Figure S1. Variation in observed Shannon diversity index for all cruises.

Figure S2. Relative abundances of the top ten most abundant OTUs found during the October 2015 transect. All OTUs were affiliated with *Prochlorococcus sp*. Colour shows interpolated relative abundances using the weighted-average gridding algorithm in Ocean Data View (http://odv.awi.de; version 4.7.8).

Figure S3. Relative abundances of the top ten OTUs exhibited the highest variance during the October 2015 transect. Colour shows interpolated relative abundances using the weighted-average gridding algorithm in Ocean Data View (http://odv.awi.de; version 4.7.8). Arrows denote hotspots in relative abundance detected for OM-1 clade *Candidatus* Actinomarina.

Figure S4. Occupancy-frequency distributions of populations binned by phyla/class during the October 2015 cruise. Bimodality tests was performed using Mitchell-Olds and Shaw's test for quadratic extremes (Mitchell-Olds and Shaw, 1987), a proxy for Tokeshi's test (Tokeshi, 1992). ND=Not Determined. Significance level is indicated with "***", "**" and"*" for p-values <0.001, <0.01 and <0.05, respectively.

Figure S5. Occupancy-frequency distributions of populations binned by phyla/class during the December 2015 and January 2016 cruises. Total, picoplankton and "large" denote size-fractionated community DNA from >0.2 µm, >0.2 and <3.0 µm and 3.0 µm filters, respectively. Bimodality tests was performed using Mitchell-Olds and Shaw's test for

quadratic extremes (Mitchell-Olds and Shaw, 1987), a proxy for Tokeshi's test (Tokeshi, 1992). ND=Not Determined. Significance level is indicated with "***", "**" and"*" for p-values <0.001, <0.01 and <0.05, respectively.

Figure S6. Occupancy-frequency distributions of OTUs affiliated with *Prochlorococcus* sp. during the October 2015 (A), and December 2015 and January 2016 cruises (B). Total, picoplankton and "large" in (B) denote size-fractionated community DNA from >0.2 µm, >0.2 and <3.0 µm and >3.0 µm filters, respectively. Bimodality tests was performed using Mitchell-Olds and Shaw's test for quadratic extremes (Mitchell-Olds and Shaw, 1987), a proxy for Tokeshi's test (Tokeshi, 1992). ND=Not Determined. Significance level is indicated with "***", "**" and"*" for p-values <0.001, <0.01 and <0.05, respectively.

Figure S7. Maximum-likelihood tree of OTUs affiliated with *Prochlorococcus* sp. exhibiting core or satellite metapopulation dynamics obtained from 16S rRNA gene data from all cruises. The evolutionary history was inferred by using the Maximum Likelihood method based on the Tamura-Nei model (Tamura and Nei, 1993). The bootstrap consensus tree inferred from 999 replicates is taken to represent the evolutionary history of the taxa analyzed (Felsenstein, 1985). Branches corresponding to partitions reproduced in less than 50% bootstrap replicates are collapsed. Initial tree(s) for the heuristic search were obtained automatically by applying Neighbor-Join and BioNJ algorithms to a matrix of pairwise distances estimated using the Maximum Composite Likelihood (MCL) approach, and then selecting the topology with superior log likelihood value. The analysis involved 18 nucleotide sequences. All positions containing gaps and missing data were eliminated. There were a total of 427 positions in the final dataset. Evolutionary analyses were conducted in MEGA7 (Kumar et al., 2016).

Table S1. Prevalence of significantly bimodal occupancy-frequency patterns in different community compartments (size fractions and taxa) in the present paper. Bimodality tests was performed using Mitchell-Olds and Shaw's test for quadratic extremes (Mitchell-Olds and Shaw, 1987), a proxy for Tokeshi's test (Tokeshi, 1992). ND=Not Determined. Significance level is indicated with "***", "**" and"*" for p-values <0.001, <0.01 and <0.05, respectively.

	October	**November**		**December**			**January**	
Community	**Total**	**Total**	**Total**	**Picoplankton**	**"Large"**	**Total**	**Picoplankton**	**"Large"**
All	YES***	YES***	YES**	YES**	NO	YES**	YES*	NO
Cyanobacteria	YES***	YES***	YES**	YES**	NO	YES*	NO	NO
Bacteroidetes	NO	NO	NO	NO	NO	NO	NO	NO
Actinobacteria	NO	NO	NO	NO	NO	NO	NO	NO
Verrucomicrobia	NO	NO	NO	ND	NO	NO	ND	NO
Alphaproteobacteria	YES***	NO	NO	NO	NO	YES*	NO	NO
Betaproteobacteria	NO	ND	ND	ND	NO	ND	ND	NO
Gammaproteobacteria	NO	NO	NO	NO	NO	NO	NO	NO
Planctomycetes	NO	NO	NO	NO	NO	NO	ND	NO
Acidobacteria	ND	ND	ND	ND	NO	ND	ND	NO
Deltaproteobacteria	NO	NO	NO	NO	NO	NO	NO	NO
Chloroflexi	NO	NO	NO	NO	NO	NO	NO	NO
Prochlorococcus sp.	YES***	YES**	YES*	YES*	NO	YES*	YES*	NO
Synechococcus sp.	NO	NO	NO	NO	NO	NO	ND	NO
SAR11 clade	YES**	YES**	NO	NO	NO	YES*	NO	NO
SAR86 clade	NO	NO	NO	NO	NO	NO	NO	NO
Aegan-169	YES***	YES**	NO	NO	NO	NO	NO	NO

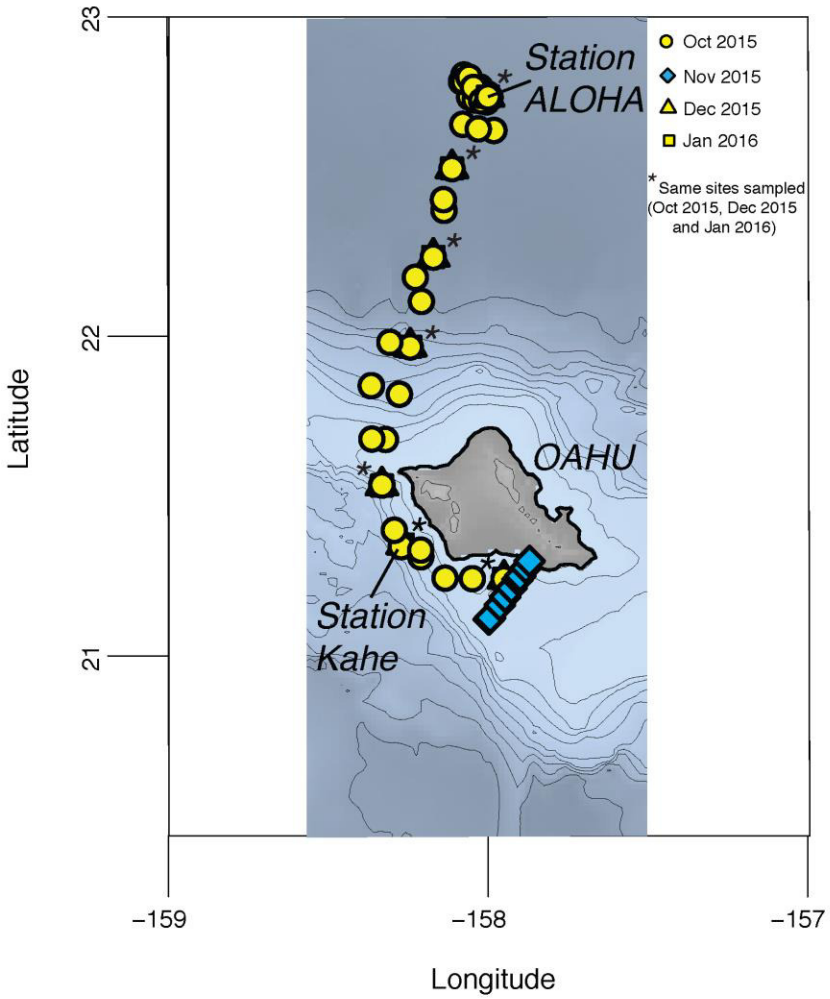

Figure 1

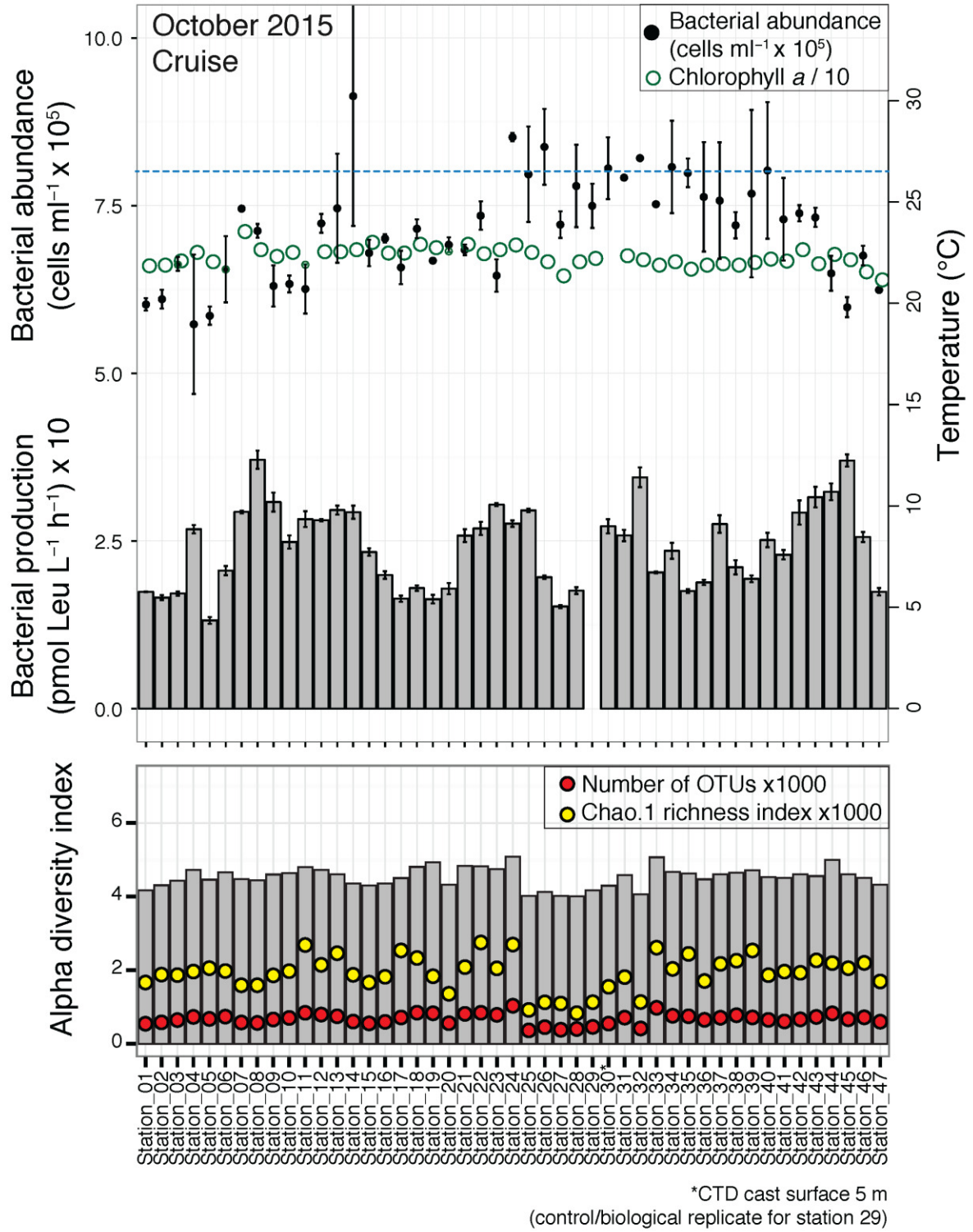

*CTD cast surface 5 m
(control/biological replicate for station 29)

Figure 2

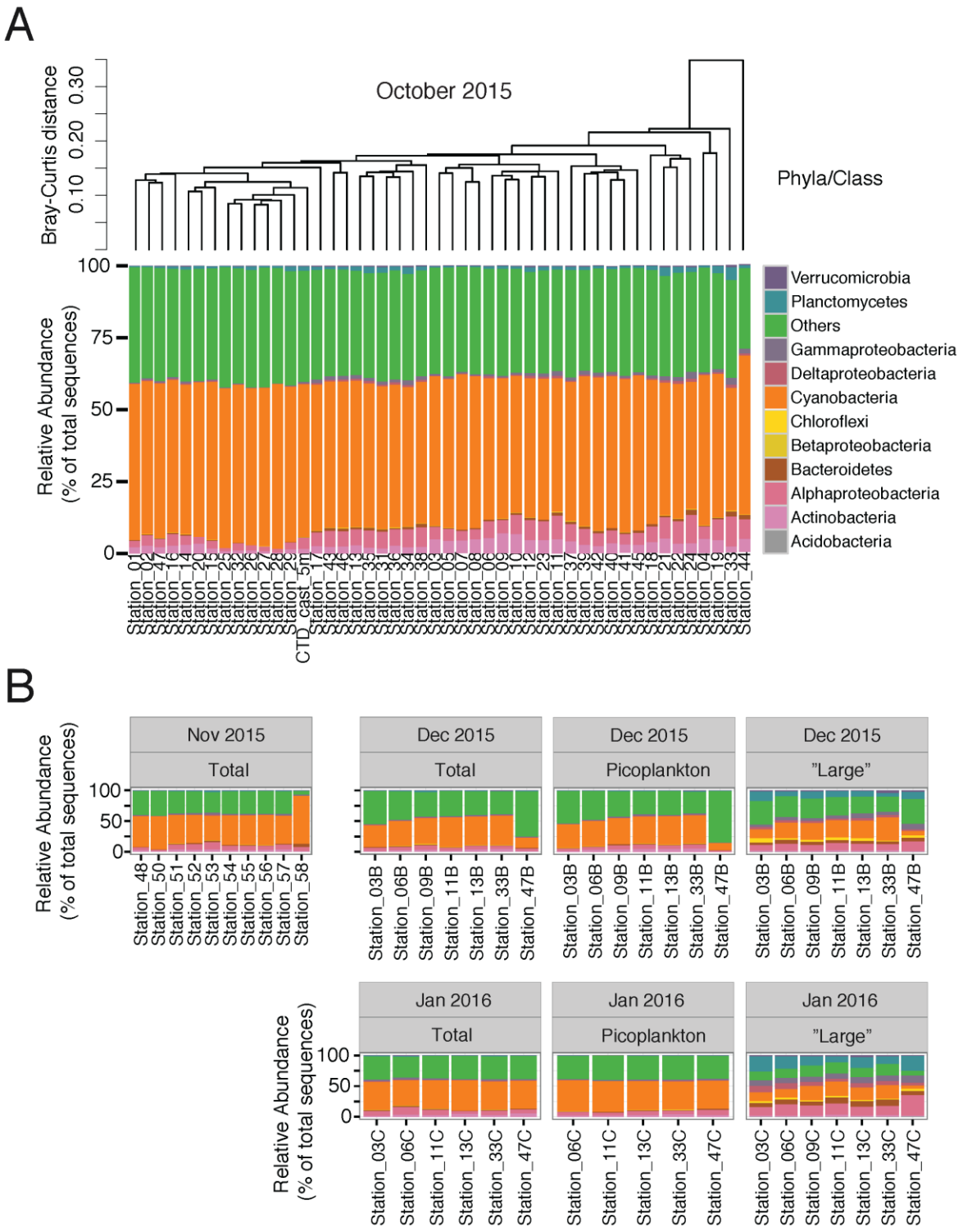

Figure 3

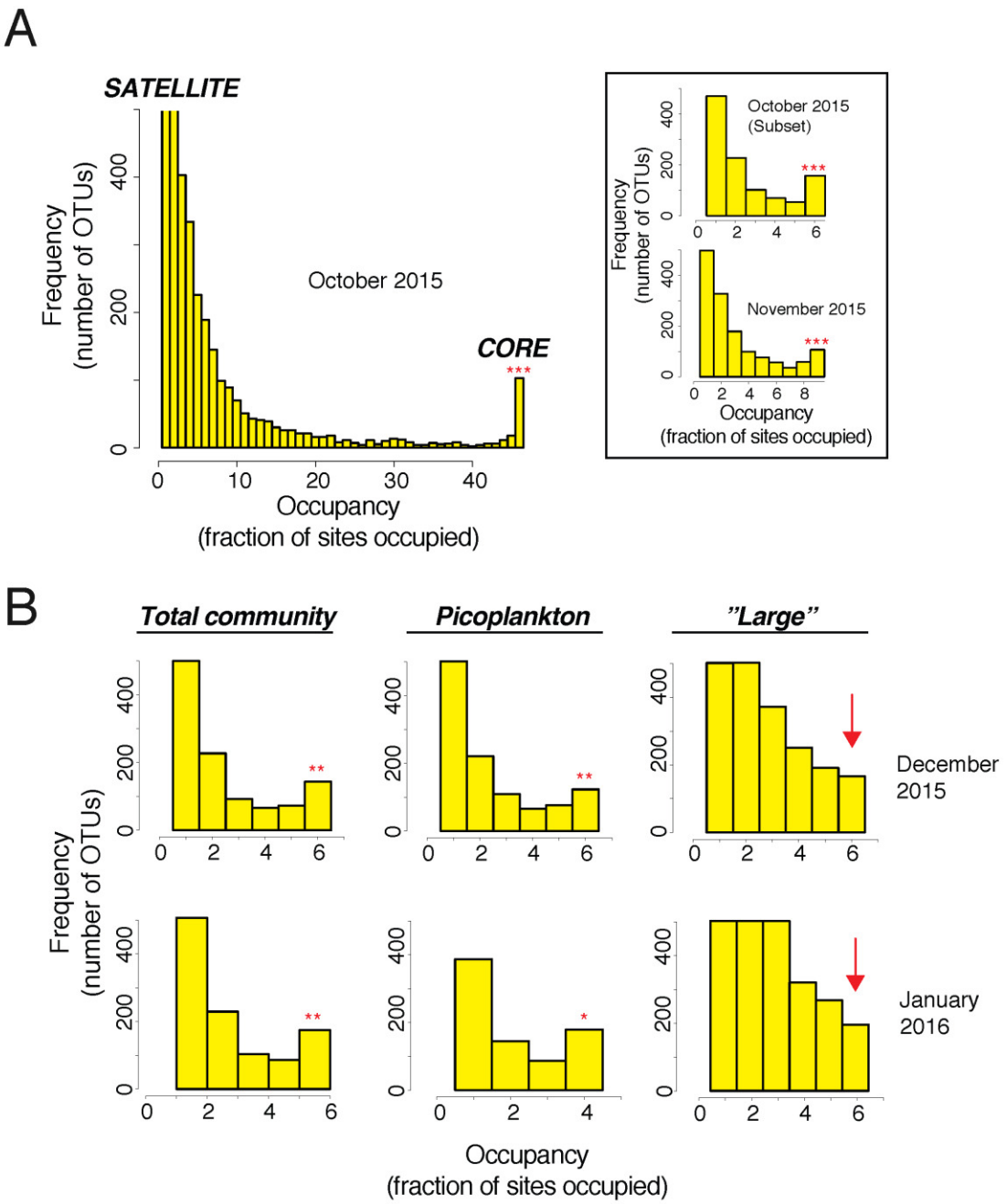

Figure 4

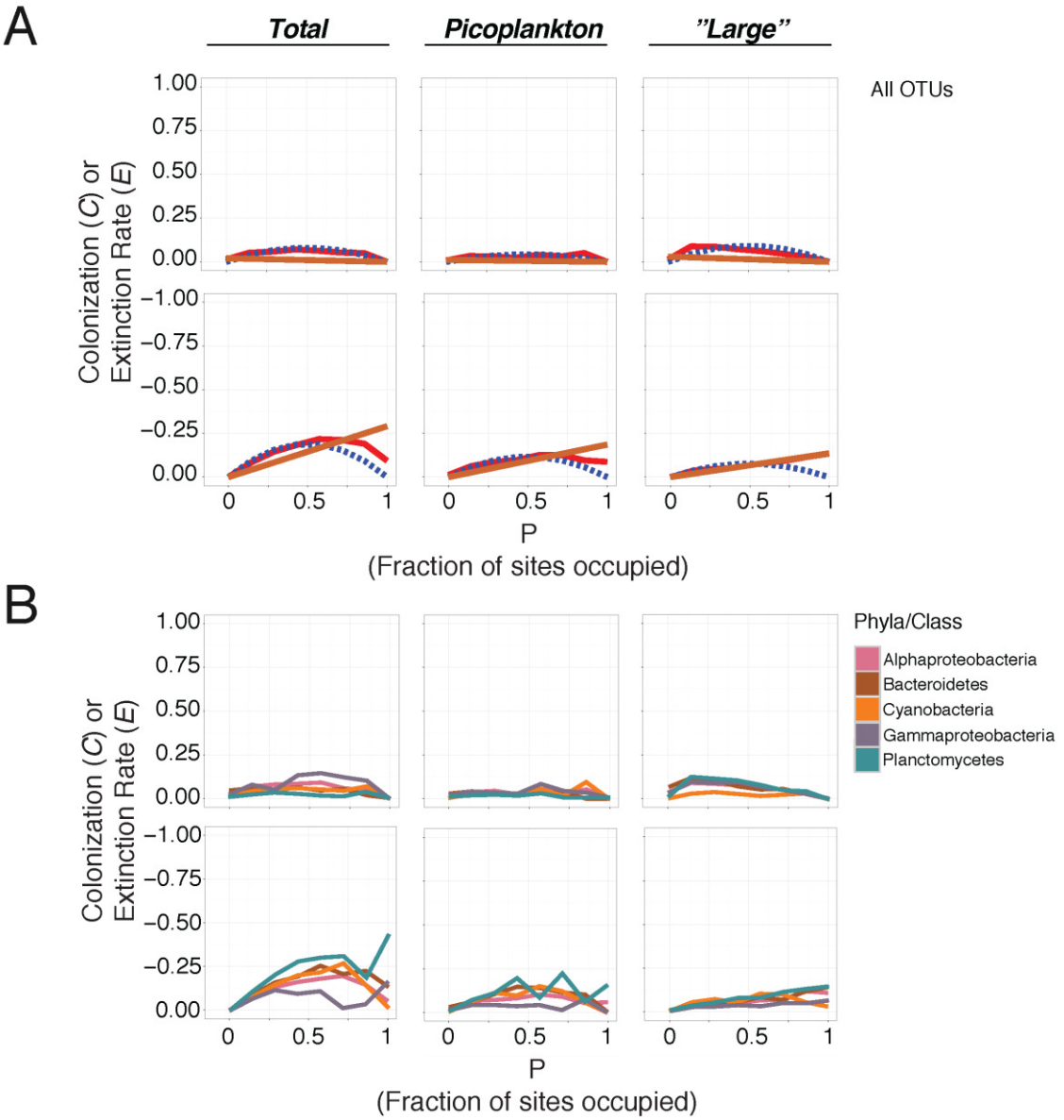

Figure 5

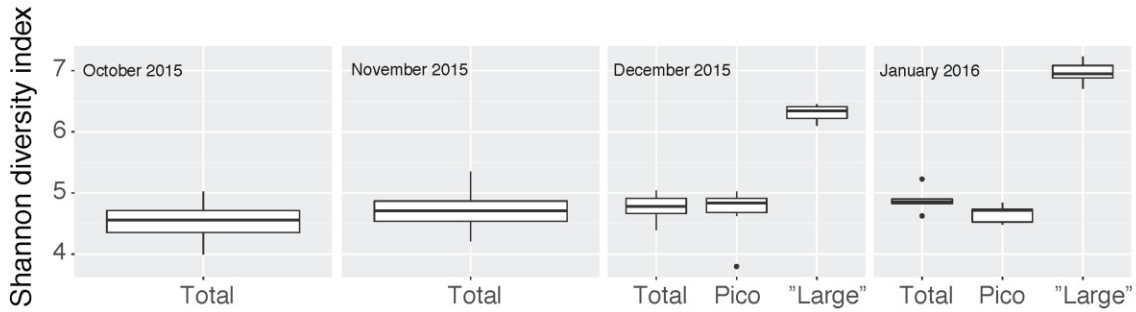

Supplementary Figure 1

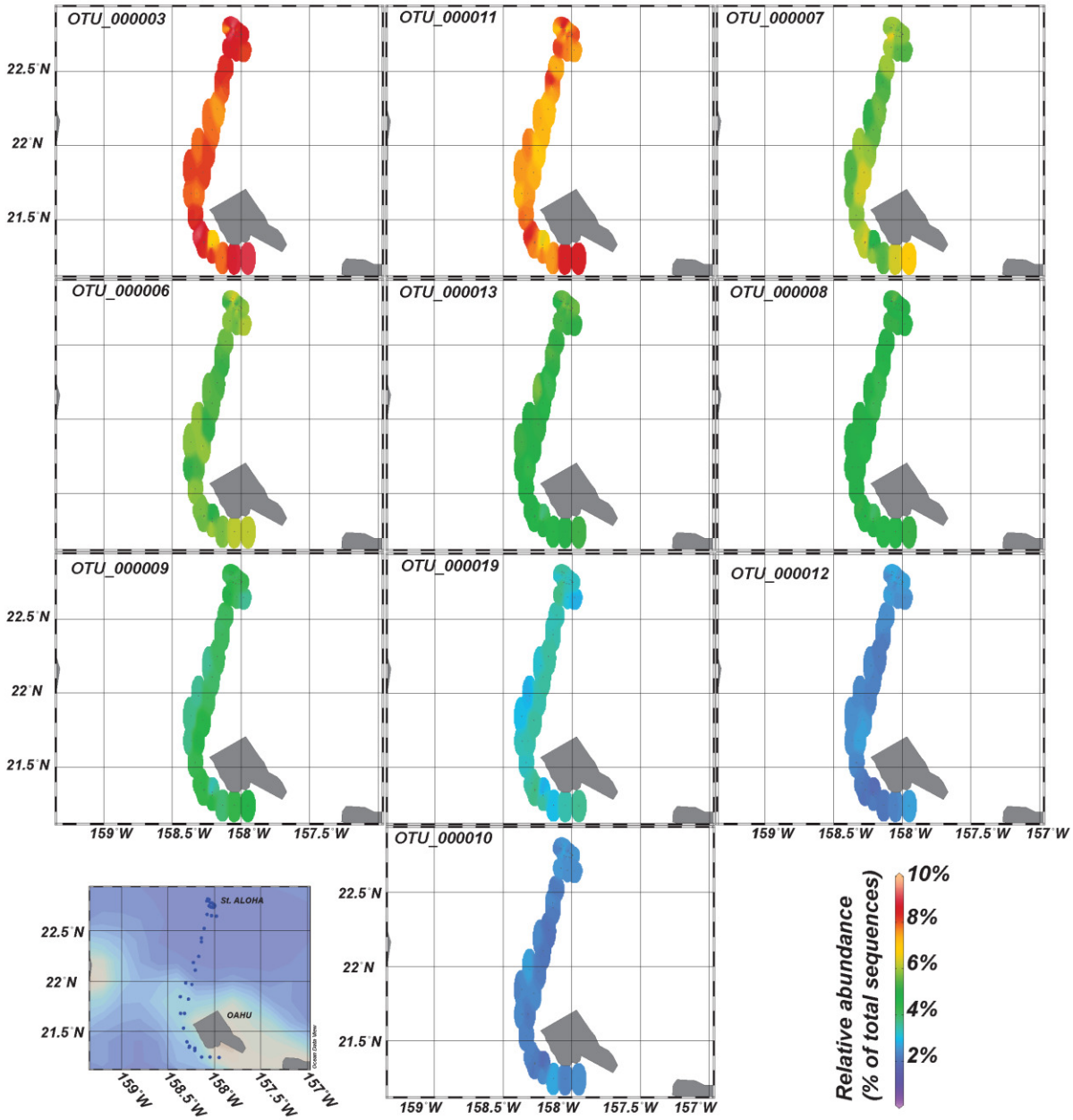

Supplementary Figure 2

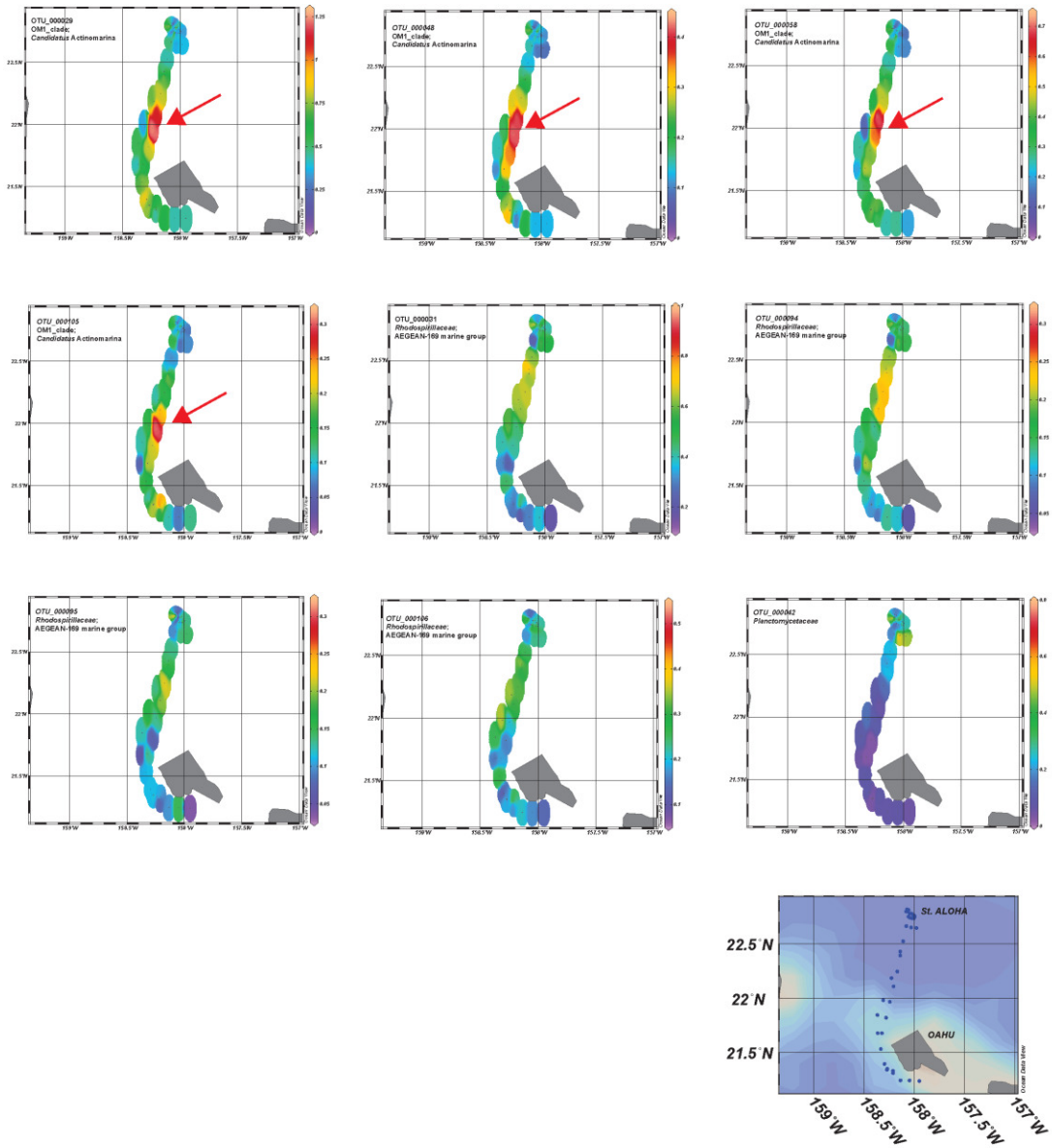

Supplementary Figure 3

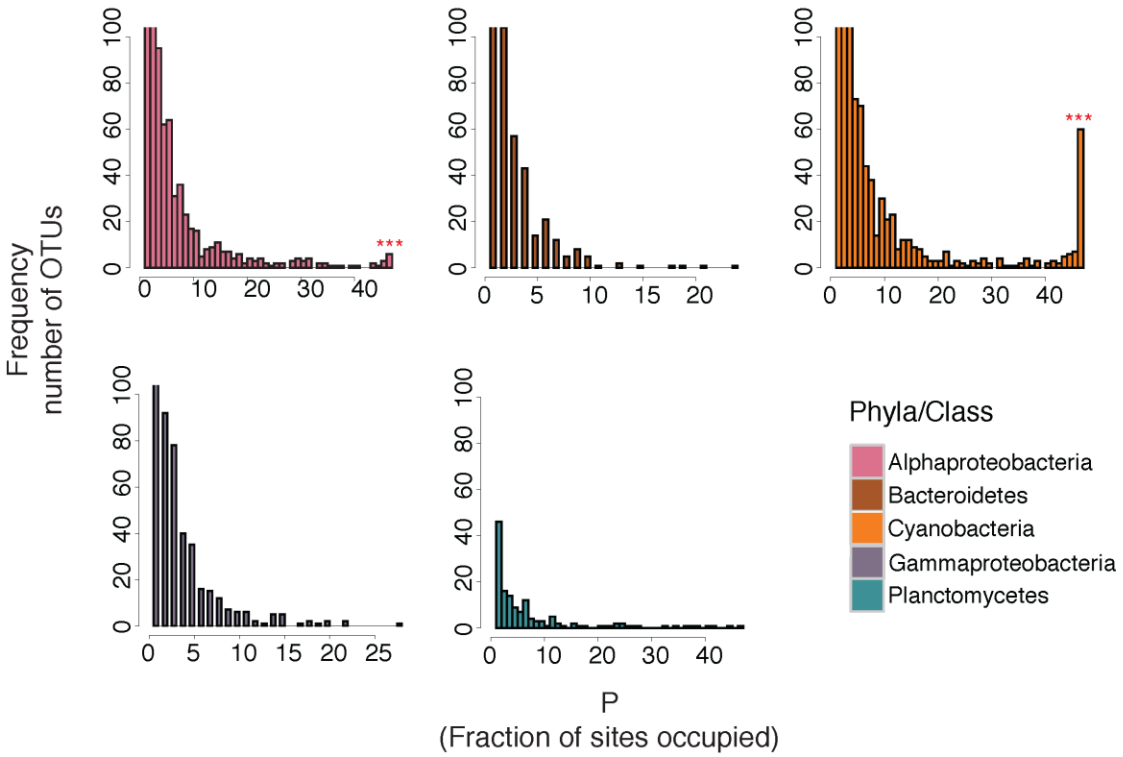

Supplementary Figure 4

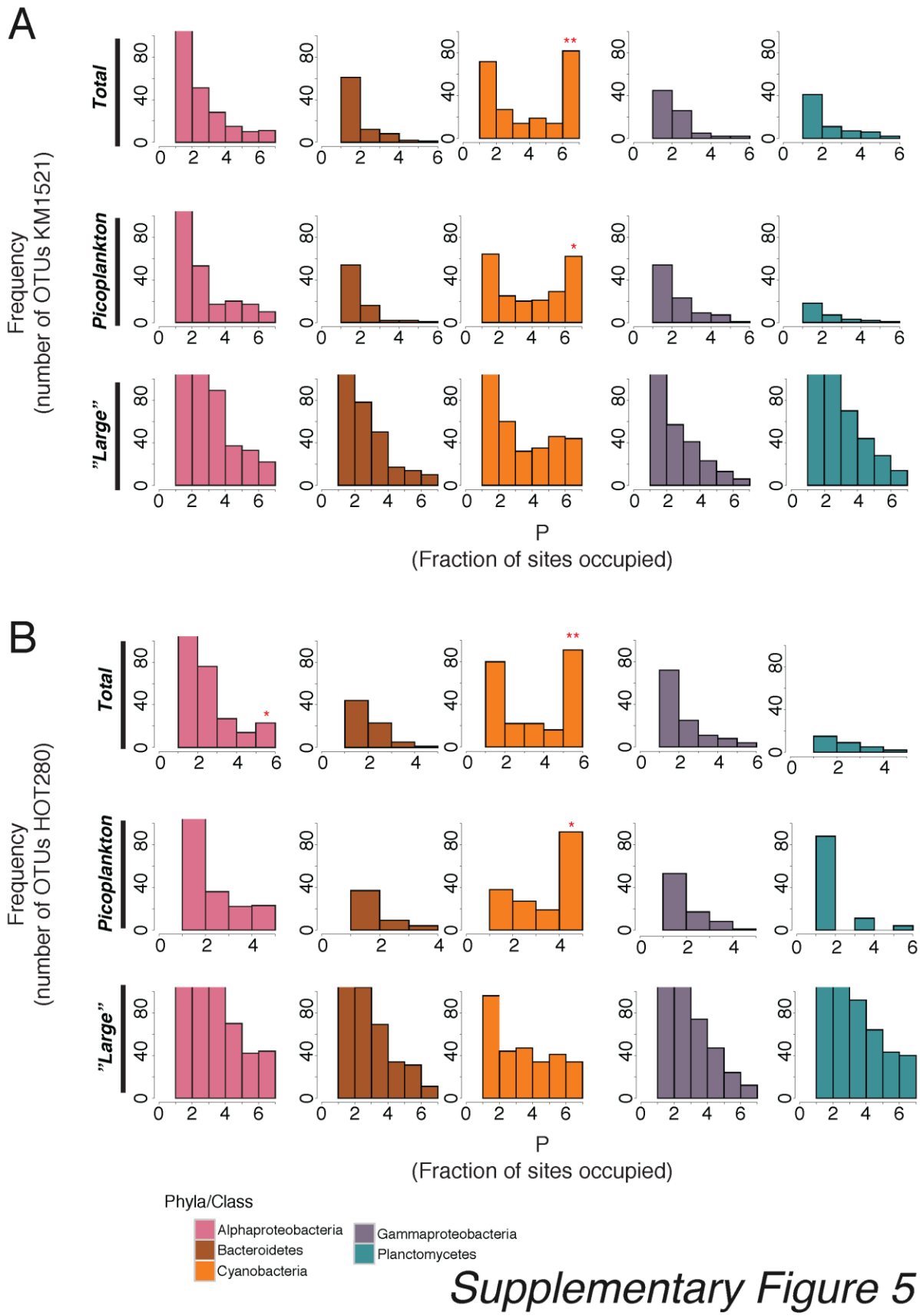

Supplementary Figure 5

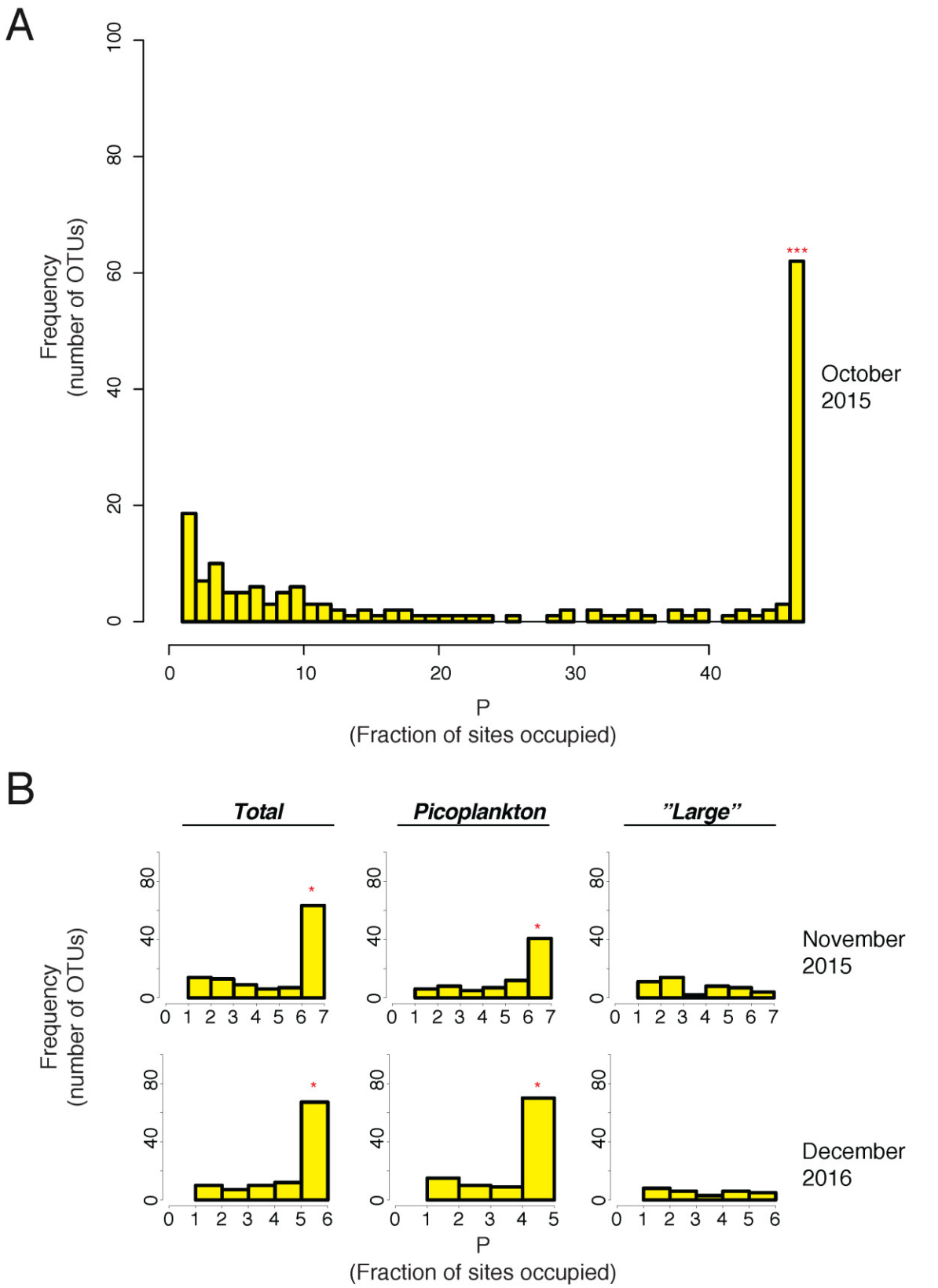

Supplementary Figure 6

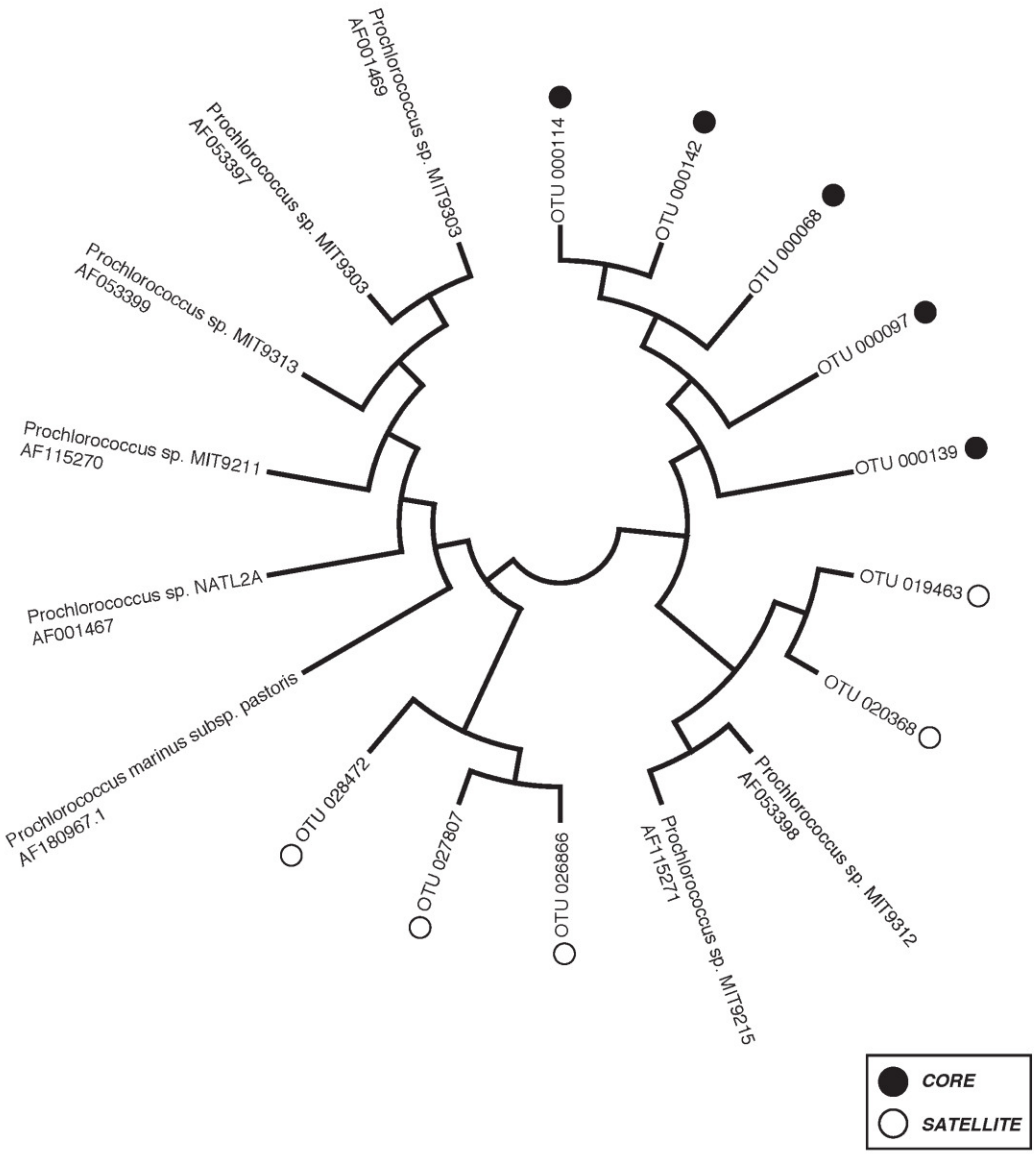

Supplementary Figure 7